Diffuse ferroelectric transition and relaxational dipolar freezing in $(Ba, Sr)TiO_3$: III. Role of order parameter fluctuations

1996 J. Phys.: Condens. Matter 8 7813

(http://iopscience.iop.org/0953-8984/8/41/024)

J. Phys.: Condens. Matter **8** (1996) 7813–7827. Printed in the UK

Diffuse ferroelectric transition and relaxational dipolar freezing in (Ba, Sr)TiO_3: III. Role of order parameter fluctuations

Neelam Singh†, Anirudh P Singh‡, Ch Durga Prasad§ and Dhanajai Pandey†

† School of Materials Science and Technology, Banaras Hindu University, Vanarasi 221005, India

‡ Shaheed Bhagat Singh College of Engineering & Technology Ferozpor 152002, India

§ Naval Materials Research Laboratory, Naval Dockyard, Bombay 400023, India

Received 10 October 1995, in final form 20 May 1996

Abstract. Results of a high-temperature x-ray powder diffraction study of the phase transition between cubic and tetragonal phases of $(Ba_{1-x}Sr_x)TiO_3$ are presented for $x = 0.08$ and 0.12 which exhibit sharp and diffuse dielectric anomalies, respectively. Experimental evidence and arguments are advanced to show that the cubic and tetragonal phases coexist over a wide range of temperatures and that this coexistence is due to the fluctuation of the order parameter which is coupled electrostrictively to strains. For $x = 0.08$, the phase coexistence disappears below the dielectric anomaly temperature T'_m, indicating the critical nature of the fluctuations. For $x = 0.12$, these fluctuations are non-critical since the phase coexistence persists even below T'_m. The complete conversion to the tetragonal phase occurs at $T_s \approx 75\,^\circ$C which is nearly $25\,^\circ$C lower than $T'_m (= 102 \pm 1\,^\circ$C). It is shown that the spontaneous polarization also increases gradually below T'_m and levels off at $T_p \approx 75\,^\circ$C. The existence of structural and polarization anomalies well below the frequency-independent dielectric anomaly temperature T'_m cannot be rationalized either in terms of the Landau-like theories for ferroelectric transitions which predict $T_s = T_p = T'_m$ or in terms of dipole glass transitions and/or relaxor ferroelectric transitions for which T'_m should be frequency dependent.

1. Introduction

Substitutional impurities are known to influence the nature of structural phase transitions in several perovskite systems. In systems such as $KMnF_3$ undergoing a fluctuation-driven first-order phase transition, the substitution of Mn by Mg or Ca can make the phase transition continuous [1, 2]. In $KTaO_3$, which is an incipient ferroelectric down to 0 K, substitutional impurities such as Li and Na in place of K, or Nb in place of Ta can induce ferroelectric-like order at low temperatures if their concentration exceeds a certain critical limit [3, 4]. The nature of the phase transition in $BaTiO_3$, when doped with substitutional impurities, appears to change from a discontinuous to a continuous type [5]. More careful analysis has, however, revealed that the apparently continuous transition is essentially due to the presence of order-parameter fluctuations which smother the discontinuity [6, 7]. In mixed systems such as (Ba, Sr)TiO_3, (Pb, La)(Zr, Ti)O_3 and (Pb, Ca)TiO_3, the temperature dependence of the dielectric constant indicates a smeared transition. Smearing increases with increasing concentration of the substitutional impurities [8–10]. It is of interest to know whether these

0953-8984/96/417813+15$19.50

broad dielectric anomalies are related to a structural phase transition or to the onset of freezing of dipolar clusters as in some orientational glasses.

In the preceding two papers [8, 11], we discussed the dielectric behaviour of $(Ba_{1-x}Sr_x)TiO_3$ ceramics with $x = 0.08$, 0.12, 0.16 and 0.20. It was pointed out that the temperature variation in the real (ϵ') and imaginary (ϵ'') parts of the dielectric constant in samples with $x \leqslant 0.12$ needs to be distinguished from that of samples with $x > 0.12$. Orientational glass behaviour was confirmed [11] for compositions with $x > 0.12$ on the basis of frequency-dependent peak temperatures T'_m and T''_m in the ϵ' and ϵ'' versus temperature T plots. T''_m is invariably lower than T'_m for such compositions. For compositions with $x \leqslant 0.12$, the temperature variation in the dielectric constant has some similarities to that of the pure system ($BaTiO_3$), e.g. thermal hysteresis during heating and cooling cycles of measurement, frequency independence of T'_m and T''_m, and the equality of T'_m and T''_m [11]. These compositions, however, exhibit several dissimilarities also compared with the pure system. For example, the ϵ' verses T plot shows a very sharp change below the transition temperature in pure $BaTiO_3$ whereas it is quite diffuse in strontium-substituted samples with $x = 0.12$. Also, the dielectric constant follows the Curie–Weiss law up to temperatures very close to T'_m in the pure system while Sr-substituted samples show a marked departure over a wider range of temperatures [8]. In addition, a low-frequency dielectric relaxation in the frequency range 10^3 Hz $\leqslant f \leqslant 10^6$ Hz appears below T'_m for all the compositions with $0.08 \leqslant x \leqslant 0.20$ [8, 11]. The relaxation time for the low-frequency relaxation follows an Arrhenius-type temperature dependence below T'_m. Such low-frequency relaxations are not observed in the pure system. It was proposed in the preceding papers [8, 11] that this low-frequency relaxation arises because the system is in a 'domain state' in the sense of Imry and Ma [12] with ferroelectric order extending over mesoscopic length scales only. For strontium concentrations $x > 0.12$, the size of these domains seems to have become too small to be stable against thermal fluctuations. This leads to a cluster-glass-like behaviour since one also observes frequency dispersion in T'_m and T''_m [3, 4].

As shown in part II of this series of papers, for compositions with $x \leqslant 0.12$, the temperature dependence of the dielectric constant shows a reasonably sharp change for $x = 0.08$ at T'_m while it is diffuse or smeared out for $x = 0.12$. The frequency independence of T'_m and T''_m for $x = 0.12$ rules out the possibility that T'_m is the freezing temperature corresponding to a dipole glass or relaxor ferroelectric transition. The question therefore arises whether the smeared $\epsilon'(T)$ response is due to a genuine thermodynamic phase transition taking place over a range of temperatures.

We present here the results of a detailed high-temperature powder x-ray diffraction (XRD) study of the crystallographic transition for compositions with $x = 0.08$ and 0.12 to understand the origin of the smeared $\epsilon'(T)$ response for $x = 0.12$. We correlate the XRD results with dielectric and polarization measurements. It is shown that the smeared dielectric response for $x = 0.12$ is due to an unusual type of order-parameter fluctuation occurring over a fairly wide range of temperatures extending from temperatures above T'_m to well below T'_m. For the composition with $x = 0.08$, the order-parameter fluctuations are observed above T'_m only in the so-called critical regime, as expected [5–7] for a fluctuation-driven first-order phase transition.

2. Experimental details

XRD studies were performed on a Rigaku rotating-anode powder diffractometer fitted with a high-temperature attachment. XRD data were collected for 111, 200 and 310 reflections

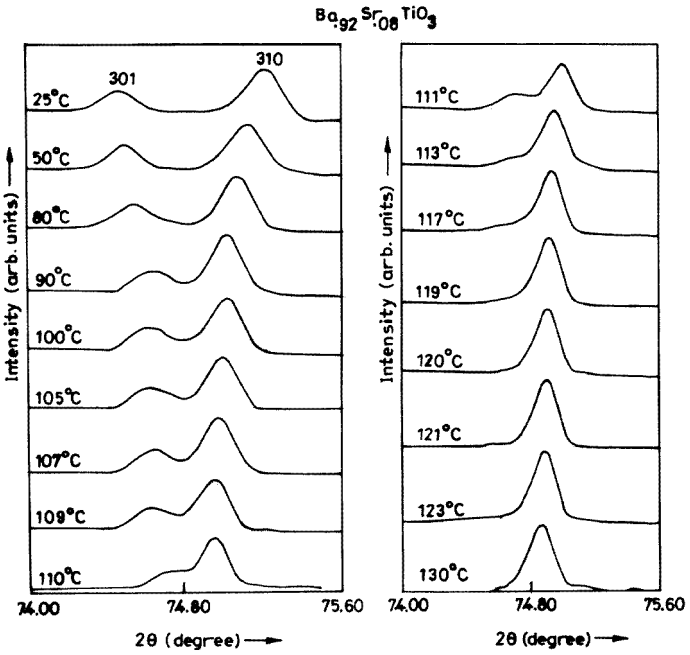

Figure 1. Evolution of the 301 and 310 reflections with temperature for $Ba_{0.92}Sr_{0.08}TiO_3$ (Ca Kα radiation).

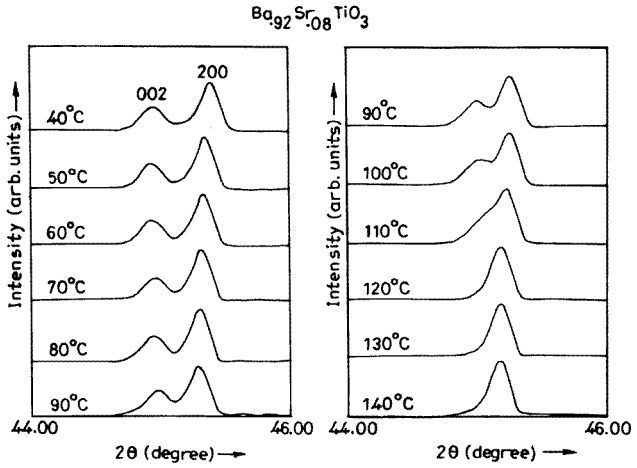

Figure 2. Evolution of the 002 and 200 reflections with temperature for $Ba_{0.92}Sr_{0.08}TiO_3$ (Cu Kα radiation).

at several temperatures for both the samples during heating cycle. Powder samples obtained after crushing sintered pellets were used for XRD studies. The preparation of pellets has already been described in part I [8] of this series. The Kα_2 contribution to XRD profiles was removed using Rachinger's method [13]. Most of the analysis on structural transition was performed using 301 and 310 pair of reflections at large angles because of better resolution.

The temperature for the high-temperature attachment was manually controlled to within $\pm 2\,^{\circ}$C.

Polarization measurements were performed using a commercial hysteresis loop tracer set-up (Digital Systems, Bombay) based on a Sawyer–Tower [14] circuit operating at a switching field frequency of 50 Hz. The sample used was 0.2 cm thick and about 1.3 cm in diameter. The dielectric measurements were carried out using a Schlumberger impedance–gain phase analyser model 1260. The sample dimensions were nearly the same as for polarization measurement. The heating and cooling rates were $1\,^{\circ}$C min^{-1} and were controlled using an Indotherm programmable temperature controller. For dielectric measurements, air-dried silver paste supplied by Elteck (Bangalore) was used for electroding. For the polarization studies, fired-on silver electrodes were applied.

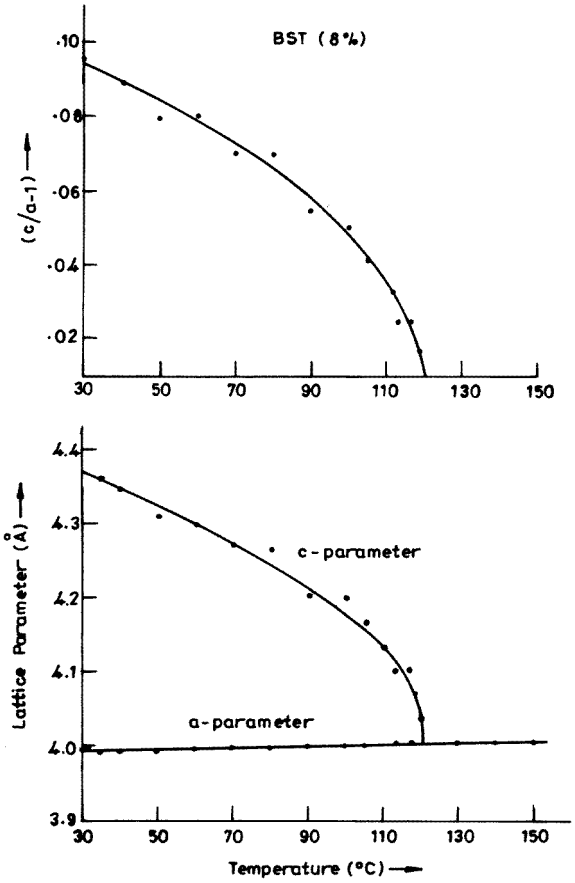

Figure 3. Variations in lattice parameters a and c and tetragonality $c/a - 1$ with temperature for $Ba_{0.92}Sr_{0.08}TiO_3$.

3. Results and analysis

3.1. ($Ba_{0.92}Sr_{0.08}$)TiO_3 sample

Figure 1 shows the evolution of the 301 and 310 profiles as a function of temperature for $x = 0.08$. It is evident from this figure that, with increasing temperature, the 301 and 310 profiles approach each other, implying lowering of the c/a ratio. These two peaks are expected to merge at some critical temperature corresponding to the tetragonal-to-cubic structural phase transition. No such merger is, however, evident from figure 1. On the contrary, the intensity of the 301 reflection starts to decrease above 109 °C without ever merging with the 310 reflection. Up to 109 °C, the ratio of the intensity of the 301 reflection to that of the 310 reflection remains nearly constant but starts to change rapidly above 109 °C. We find that the 301 peak is identifiable up to 120 °C after proper magnification of the profiles. Some residual intensity, however, persists in the same 2θ region at still higher temperatures. For the 002–200 pair of reflections, the residual scattering is not so well resolved because of the smaller $\Delta(2\theta)$ separation of this pair of reflections. However, even for this pair, distinct asymmetry at the smaller-angle end of the profiles persists up to 140 °C which points towards the presence of extra scattering at the smaller-angle tail of the profiles (figure 2).

The temperature variation in unit-cell parameters a and c and tetragonality ($\eta = c/a - 1$), as obtained from the positions of the 301 and 310 reflections, is shown in figure 3. As can be seen from this figure, the parameter c decreases in a nearly linear fashion with increasing temperature up to abut 110 °C. Beyond 110 °C, the fall in c is more rapid. On the contrary, the parameter a changes only marginally with increasing temperature in the whole temperature range. Even at 120 °C, up to which the 301 peak was somewhat identifiable, c does not coincide with a. As a result of this, the temperature of the tetragonal-to-cubic transition remains indistinct.

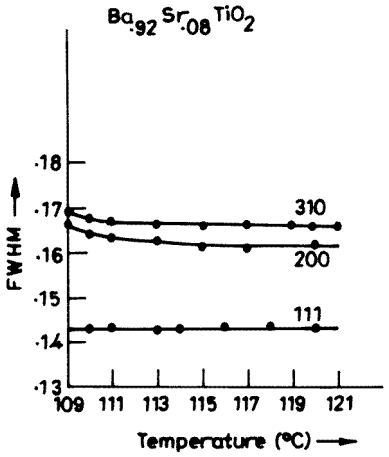

Figure 4. Temperature variations in the FWHMs of 310, 200 and 111 reflections of $Ba_{0.92}Sr_{0.08}TiO_3$ above T'_m.

Figure 4 depicts the temperature variation in the full width at half-maximum (FWHM) of the 310, 200 and 111 profiles above 109 °C. The FWHM of the 310 and 200 profiles continuously decreases with increasing temperature and levels off (within the resolution

limit of our diffractometer) at around 120 °C. The FWHM of the 111 profile, however, remains nearly constant at all temperatures.

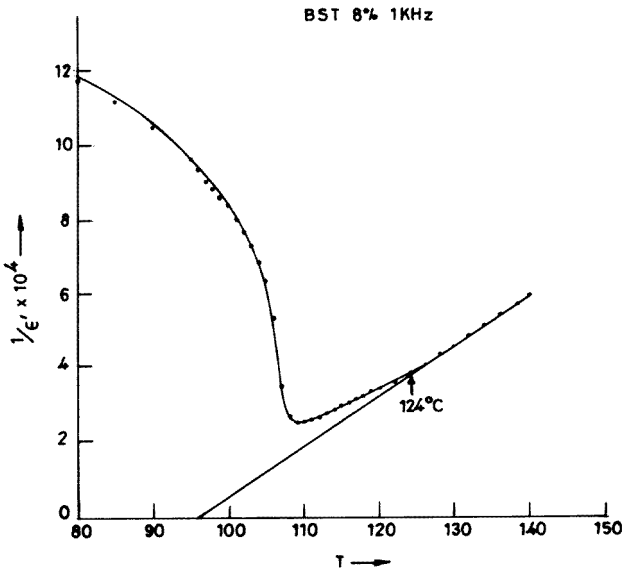

Figure 5. Variation in dielectric stiffness $1/\epsilon'$ with temperature for $Ba_{0.92}Sr_{0.08}TiO_3$. Note the departure from Curie–Weiss behaviour below 124 °C.

These observations suggest the existence of two characteristic temperatures: firstly $T = 109 \pm 1$ °C above which the intensity anomaly appears and the slope of the temperature variation in c changes, and secondly $T = 120 \pm 2$ °C at which the FWHM of the 310 and 200 reflections levels off within the limits of our experimental resolutions. At the second characteristic temperature, the extrapolated value of c seems to coincide with a (see figure 3). It is interesting to note that the first characteristic temperature coincides with the temperature T_m' of the dielectric anomaly for the heating cycle as can be seen from figure 5 which depicts the temperature variation in dielectric stiffness $1/\epsilon_r'$. As shown in figure 5, a departure from the Curie–Weiss law occurs at around 124 °C, which interestingly is close to the second characteristic temperature at which the tetragonality seems to vanish. The Curie–Weiss critical temperature $T_0 (= 90$ °C) is lower than the ϵ' peak temperature of 109 °C, as expected for a first-order phase transition. The Curie–Weiss constant C' is found to be 3.09×10^{-6} K.

3.2. $(Ba_{0.88}Sr_{0.12})TiO_3$ sample

The evolution of the 301 and 310 profiles with temperature for samples containing 12 at.% Sr is shown in figure 6. It can be seen from this figure that the 301 and 310 reflections shift towards each other with increasing temperature. However, above 75 °C, the intensity of the 301 reflection starts to decrease as a result of which the peak position of this reflection is identifiable only up to 87 °C although some residual intensity in the same 2θ region persists up to fairly high temperatures. A similar feature is observed for the 002 and 200 pair of reflections; the intensity of the 002 reflection starts to decrease above 75 °C but the persistence of this reflection up to very high temperatures can be inferred from the

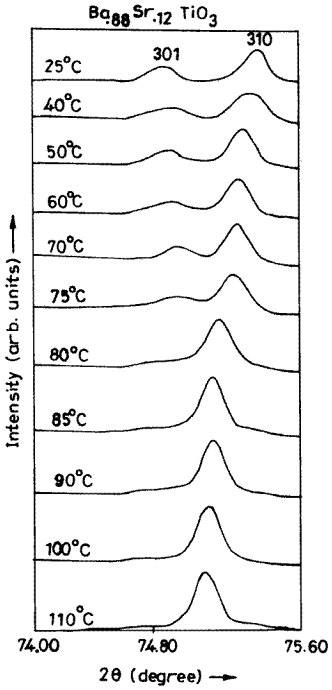

Figure 6. Evolution of the 301 and 310 reflections with temperature for $Ba_{0.88}Sr_{0.12}TiO_3$ (Cu Kα radiation).

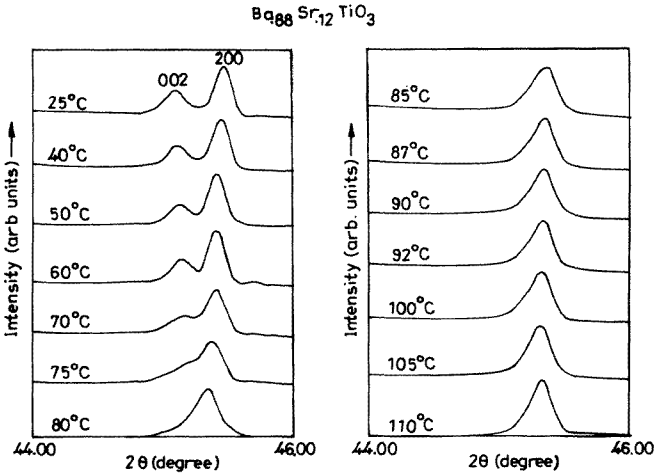

Figure 7. Evolution of the 002 and 200 reflections with temperature for $Ba_{0.88}Sr_{0.12}TiO_3$ (Cu Kα radiation).

asymmetry at the small-angle end of the 200 profile (figure 7).

The temperature variations in the lattice parameters and η, calculated from the 301 and

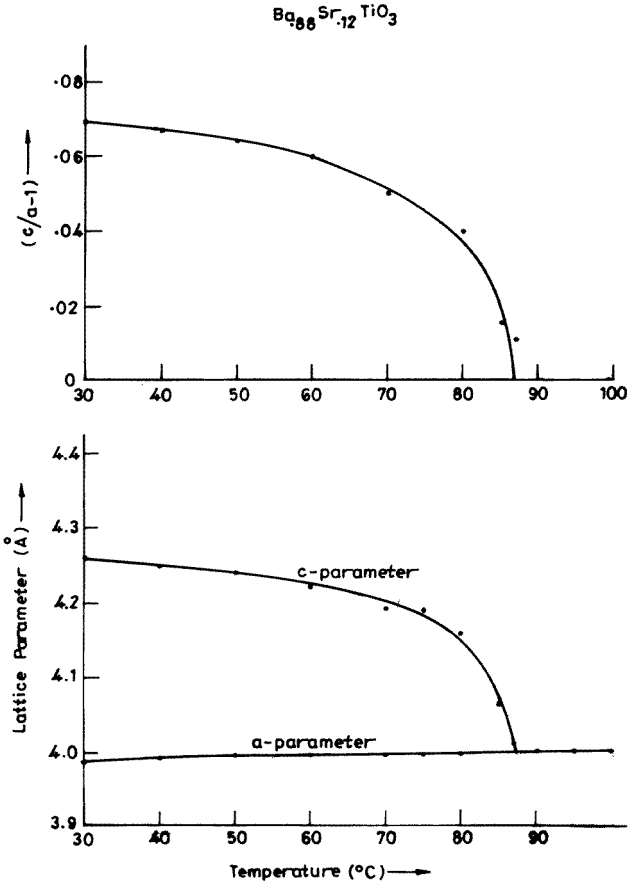

Figure 8. Variation in the lattice parameters a and c and tetragonality $c/a - 1$ with temperature for $Ba_{0.88}Sr_{0.12}TiO_3$ (Cu Kα radiation).

310 peak positions, are shown in figure 8. It is easy to see from this figure that the slope of the c versus temperature plot changes considerably at around 80 °C and, on extrapolation, c is expected to coincide with a at around 88 °C.

Figure 9 gives the FWHMs for the 111, 200 and 310 reflections as functions of temperature from 85 to 110 °C. The FWHM for the 111 reflection is nearly temperature independent. For the 200 and 310 reflections, the FWHMs decrease continuously with increasing temperature and level off at around 101 ± 2 °C, within the limits of the experimental resolution.

Figure 10 shows the temperature variation in the saturation polarization P_s and dielectric constant ϵ' for the same composition in both heating and cooling cycles. A comparison of figure 10 with figures 6–9 clearly reveals that the temperature at which the intensity of the 301 reflection drops off suddenly (about 75 °C) is close to the temperature at which P_s starts to fall. Around the same temperature, the tetragonality also decreases sharply. We find that the area within the hysteresis loop (P_s versus E) decreases gradually above 75 °C and the loop becomes very narrow, as shown in figure 11 for $T = 90$ °C. This type of extremely narrow hysteresis loop with gradually decreasing value of P_s persists up to about 120 °C.

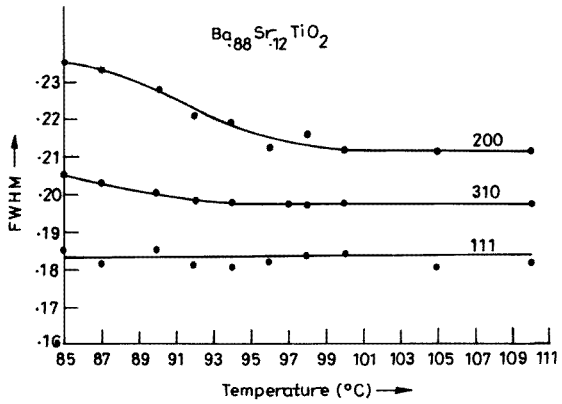

Figure 9. Variation in the FWHMs of the 200, 310 and 111 reflections of $Ba_{0.88}Sr_{0.12}TiO_3$ with temperature (Cu Kα radiation).

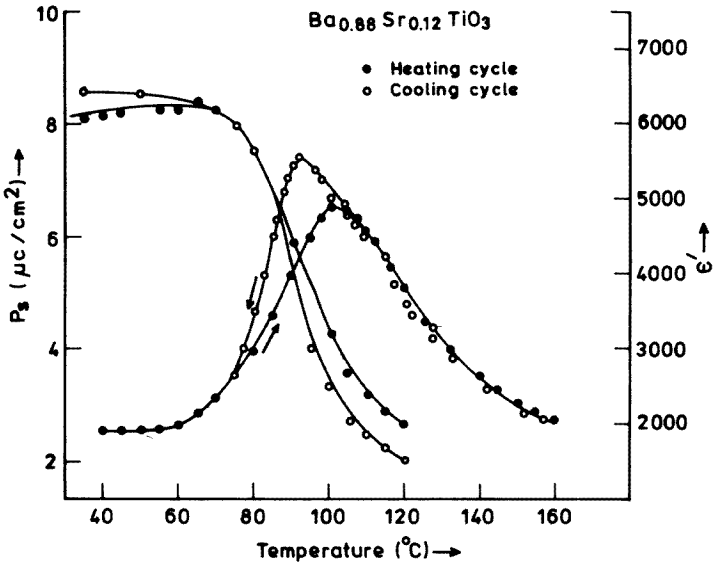

Figure 10. Variation in remanent polarization P_r and dielectric constant ϵ' with temperature for $Ba_{0.88}Sr_{0.12}TiO_3$ for heating and cooling cycles.

Above 120 °C, the loop area suddenly increases and the shape becomes elliptical which is characteristic of a lossy dielectric. As such, it was not possible to verify the presence or absence of polarization above 120 °C using our hysteresis loop set-up. It may be noted that the basic trends of the P_s versus T curves for heating and cooling cycles are similar even though the absolute values differ slightly. The dielectric constant ϵ' shows considerable hysteresis in the heating and cooling, possibly owing to the first-order nature of the phase transition. It is interesting to note that the temperature at which the FWHMs of the 200 and 310 reflections level off in the heating cycle is close to the dielectric constant peak temperature $T'_m = 102 \pm 1$ °C for the heating cycle as can be seen from a comparison of

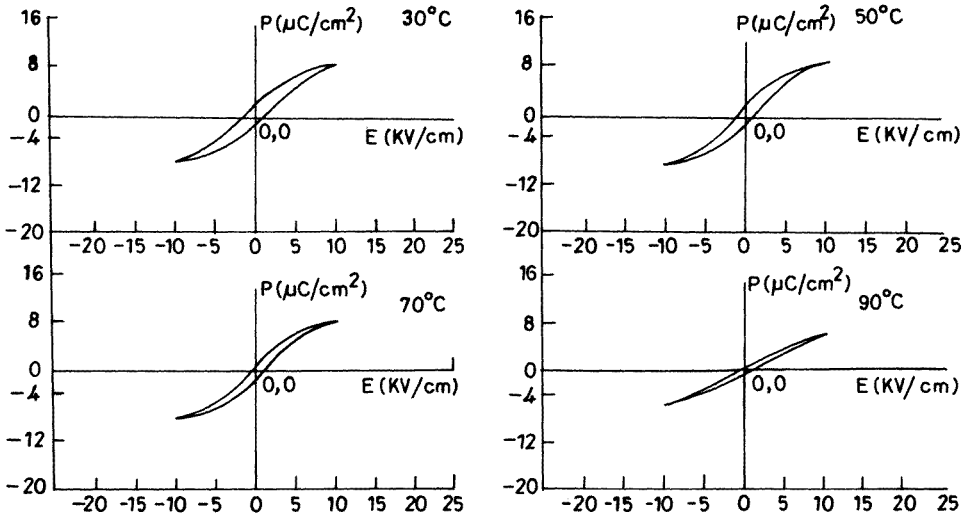

Figure 11. Hysteresis loops for $Ba_{0.88}Sr_{0.12}TiO_3$ at 30, 50, 70 and 90 °C.

figure 6 with figure 10. Since XRD measurements could not be made for the cooling cycle, it is not possible to correlate $\epsilon'(T)$ for the cooling cycle with structural changes. We do not, however, anticipate any marked difference in the trend except for some thermal hysteresis.

4. Discussion of results

It is evident from the foregoing that the crystallographic tetragonal-to-cubic transition temperatures in $(Ba_{1-x}Sr_x)TiO_3$ for $x = 0.08$ and 0.12 are indistinct and do not coincide with the temperatures T'_m at which ϵ' has its maxima. For 8 at.% Sr, the crystallographic transition temperature is higher than T'_m while, for 12 at.% Sr, it is lower than T'_m. As mentioned earlier, the nature of the temperature variation in the dielectric constant also changes from a sharp response with thermal hysteresis typical of a first-order phase transition for $x = 0.08$ to a diffuse or smeared-out response for $x = 0.12$ with some hysteresis. It may be noted that the thermal hysteresis reported in [11] for $T > T'_m$ was an artefact of improper thermal equilibriation in the cooling cycle. With better thermal equilibriation in the cooling cycle, we find that the thermal hysteresis persists below T'_m only (see figure 10) as expected for a first-order phase transition. We shall now discuss the implications of our high-temperature XRD results in order to understand the difference between the natures of the dielectric responses for $x = 0.08$ and 0.12.

4.1. Structural transition aspects

4.1.1. $Ba_{0.92}Sr_{0.08}TiO_3$. We shall first try to understand the implications of the intensity anomaly for the 301 and 310 pair of reflections above T'_m ($= 109 \pm 1$ °C) for 8 at.% Sr substitution. For a pure tetragonal structure, the intensity of the 301 reflection is roughly half the intensity of 310 as can be seen from figure 1 for temperatures below T'_m. Above $T_{m'}$ the intensity of the 301 reflection gradually decreases with increasing temperature and is invariably much less than half the intensity of the 310 reflection. This clearly indicates

the existence of another phase which scatters x-rays more or less at the position as that of the 310 reflection of the tetragonal phase.

The negligibly small variation in a of the tetragonal phase with temperature without any observable anomaly near T_m' clearly suggests that its value is nearly equal to the cell parameter for the cubic phase. As a result, the 310 reflection of the cubic phase will be superimposed on the 310 reflection of the tetragonal phase. Thus the intensity anomaly for the 301 and 310 pair of reflections above T_m' implies the coexistence of the tetragonal and cubic phases. When the matrix is fully tetragonal, the ratio of the intensity of the 310–130 reflection to that of 301 is nearly two. As the volume fraction of the cubic phase increases with increasing temperature above T_m', this ratio becomes greater than two. Finally, when the entire matrix is cubic, the 301 reflection will disappear. However, the presence of weak residual scattering around the 301 position up to temperatures well above T_m' suggests the persistence of tetragonal clusters even at these temperatures. Viewed from a higher temperature above T_m', the extra scattering around the 301 position indicates a precursive (pre-transitional) phenomenon related to the cubic-to-tetragonal phase transition.

The phase coexistence above T_m' can in principle be attributed to the presence of frozen-in compositional inhomogeneities in solid solution systems. In the presence of compositional inhomogeneities, different regions of the sample can transform at different temperatures because of the dependence of the transition temperature on local composition. Therefore, there can be transformed (tetragonal) and untransformed (cubic) regions coexisting over a range of temperatures called the Curie range. The Curie range will depend on the sensitivity of the local transition temperature to the composition. This type of T_c-distribution model [15, 16] due to composition inhomogeneities predicts that firstly the Curie range extends from below T_m' to above T_m' and secondly that there is no sharp change in $\epsilon'(T)$ below T_m'. The facts that firstly the coexistence disappears abruptly at T_m' and secondly that the $\epsilon'(T)$ response for $Ba_{0.92}Sr_{0.08})TiO_3$ is not diffuse or smeared out across T_m' clearly rule out the possibility that the phase coexistence is due to the presence of frozen-in compositional inhomogeneities. In fact, as pointed out in part I [8], our samples are expected to be free from such inhomogeneities since they were prepared by a semiwet route which ensures a unit-cell level homogeneous distribution of Ba and Sr in the matrix.

Precursor clusters of the low-temperature tetragonal phase in the high-temperature cubic regime as order-parameter fluctuations have been reported in pure $BaTiO_3$ also [15]. The order-parameter fluctuations are known to be critical for pure $BaTiO_3$. The coexistence of the cubic and tetragonal phases in $(Ba_{0.92}Sr_{0.08})TiO_3$ also seems to be due to critical order-parameter fluctuations since it is firstly restricted to the temperature range over which one observes departure from the Curie–Weiss behaviour and secondly abruptly disappears below T_m'. The order-parameter fluctuations imply the appearance and disappearance of polar (tetragonal) clusters in the cubic matrix as thermal fluctuations. When the temperature is relatively high compared with T_m', the lifetime and the size of the fluctuating polar clusters will be small. As the temperature approaches T_m' from above, both the size and the lifetime of the fluctuating polar clusters are expected to increase. In a time- and space-averaged picture, such as that provided by XRD, this will show up as increasing volume fraction of the tetragonal phase in the cubic matrix on approaching T_m' from a higher temperature.

We can also rationalize the critical nature of the broadening of the x-ray profiles on approaching T_m' from a higher temperature in terms of the order-parameter fluctuations. In principle, the broadening of powder XRD profiles could be due to the presence of small coherently scattering domains and/or strains in the powder crystallites. Viewed from a temperature higher than T_m' the increases in the FWHMs of 310 and 200 reflections cannot be attributed to the domain size effect since this implies that the size of the fluctuating

polar clusters decreases on approaching T_m', which is not expected. The polar clusters present above T_m' represent a small tetragonal distortion of the cubic phase. The strain x_{ij} so produced is known [6] to be electrostrictively coupled to the polarization, i.e. $x_{11} = x_{22} = Q_{12}P_3^2$ and $x_{33} = Q_{11}P_3^2$, taking [001] as the direction of polarization. Spatial fluctuation of the order parameter can lead to an inhomogeneous distribution of the electrostrictive strains, which can in turn lead to broadening of the Bragg profiles. We expect the soft-mode picture for pure $BaTiO_2$ to be valid in the presence of 8 at.% Sr substitution also. Because of the continued softening of the optical phonons with decreasing temperature from above T_m', the effective dipole moment of the precursor polar clusters is expected to increase. This will in turn increase the electrostrictive strain and hence the FWHM on approaching T_m' from above. This strain broadening is anisotropic as can be seen from figure 4 and does not affect the 111 reflection presumably because the unit-cell volume is not changed by the onset of polarization, as is known for pure $BaTiO_3$ also [5].

The sharp dielectric anomaly with characteristic thermal hysteresis in $\epsilon'(T)$ for heating and cooling cycles points towards the first-order nature of the phase transition at T_m' for 8 at.% Sr substitution. However, owing to the extensive fluctuation regime leading to the persistence of tetragonal clusters well above T_m', the discontinuous change in the lattice parameters at T_m' is masked. This is thus the case of a fluctuation-driven first-order phase transition. The discontinuous change in the lattice parameter for $BaTiO_3$ is not masked by order-parameter fluctuations because of the extremely narrow critical regime. A similar conclusion has recently been drawn by Darlington and Cernik [6] for strontium contents up to 10 at.% based on purely XRD work without any dielectric investigations. Fluctuation-driven first-order phase transitions have also been reported for $KMnF_3$-type perovskites in the presence of impurities [1].

4.1.2. $Ba_{0.88}Sr_{0.12}TiO_3$. In contrast with the case of 8 at.% Sr substitution, where the order-parameter fluctuations are critical in nature as indicated by the disappearance of the intensity anomaly at T_m', the intensity anomaly for $(Ba_{0.88}Sr_{0.12})TiO_3$ samples disappears at a temperature which is nearly 25 °C lower than T_m'. The fact that the FWHMs of the 200 and 310 reflections remain almost temperature independent above T_m', within our experimental resolutions, suggests that the precursor polar clusters, if present at $T > T_m'$, are rather small in size and their effective dipole moments are too small to produce any detectable change in FWHM via electrostrictive coupling. The FWHM of these reflections continues to increase below T_m', which indicates the increase in the magnitude of the order parameter below T_m'. Further, the enhancement of the scattered intensity at the 301 position with decreasing temperature below T_m' implies that the volume fraction of the polar clusters is also increasing at the cost of the cubic phase. Somewhere between 75 and 80 °C, the entire matrix seems to have become tetragonal as evidenced by the disappearance of the intensity anomaly. The intensity of the 301 reflection and the remanent polarization both increased in proportion to the volume fraction of the tetragonal phase below T_m'. Both these attain saturation when the entire matrix is fully tetragonal below 80 °C. Thus, for 12 at.% Sr substitution, the transition between the cubic and tetragonal phase is quite diffuse and occurs over a wide temperature range of nearly 25 °C below T_m'. As a result of the gradual transformation of the cubic phase to tetragonal below T_m', the dielectric constant does not show a sharp anomaly below T_m' but exhibits a diffuse or smeared-out response. To our knowledge, this is the first unambiguous and direct structural evidence of a diffuse phase transition in compositionally modified $BaTiO_3$ and other related materials. As pointed out earlier, this diffuse phase transition is not caused by compositional inhomogeneities [15, 16], since

the samples were prepared by a semiwet route which yields compositionally homogeneous materials as confirmed by the x-ray line-broadening analysis presented in part I [18]. It bears a striking resemblance to the martensitic transitions where the difference between M_s (the martensite start temperature) and M_f (the martensite finish temperature) can be very wide owing to the strongly first-order character of the phase transition [18].

The Landau-like theories for $BaTiO_3$ and other similar materials predict that the temperature T_m' at which the dielectric constant shows an anomaly should be coincident with the temperature T_p at which the order parameter changes discontinuously. The temperature T_s of crystallographic transition between cubic and tetragonal phases also coincides with T_m' and T_p. This situation seems to be valid for 8 at.% Sr substitution where complete conversion to the tetragonal phase occurs at T_m'. However, for higher Sr contents, such as 12 at.%, $T_s < T_m'$ and there is no discontinuous change in the order parameter at any of these temperatures. The order parameter increases gradually and levels off at a temperature which is close to T_s at which the entire sample is tetragonal. Unlike the situation in the pure system as well as in compounds containing smaller amounts of Sr (8 at.% or less), where the fluctuation state exists above T_m' only, in mixed systems with a higher Sr content (12 at.%), the fluctuation state persists even below T_m' over a wide temperature range, as can be inferred from the increasing FWHMs of the 200 and 310 reflections below T_m' (see figure 9). These unusual features cannot be rationalized in terms of the usual Landau theory since this theory is not valid for large fluctuations in the order parameter with strong electrorestrictive coupling to the strain. To our knowledge, no satisfactory theory exists for such complex systems with large fluctuations of the coupled order parameter. One does not know therefore whether T_m', T_p and T_s should necessarily be coincident for such complex systems in the presence of large fluctuations of the coupled order parameters as evidenced by the temperature dependence of the FWHM of the XRD profiles. For the lower Sr concentration (8 at.%), these fluctuations are not pronounced enough to invalidate the predictions of the Landau theory about $T_m' = T_s = T_p$. It is, however, clear that, for mixed systems with higher impurity contents, structural and polarization anomalies may occur at temperatures well below the frequency-independent dielectric anomaly temperature. This may be a typical characteristic of systems undergoing a diffuse or smeared type of phase transition. It may be mentioned that smeared or diffuse transitions observed in relaxor ferroelectrics or dipole glasses [3, 4, 19] are different from the present situation since T_m' in the latter is frequency dependent because of which the possibility that T_m' is a thermodynamic phase transition temperature is ruled out.

4.1.3. Correlation with dynamical aspects. The discussion in the previous section was centred round the phase transition aspects for both 8 and 12 at.% Sr substitutions. The presence of low-frequency dielectric loss peaks below the frequency-independent T_m' with Arrhenius-type relaxational freezing behaviour, as discussed in part II [11], cannot, however, be reconciled in terms of the phenomenological picture given in the previous section. To correlate the structural transition and dynamical aspects, the microscopic origin of the precursor polar order above T_m' needs to be investigated. For pure $BaTiO_3$, it is usually related to the crossover from the displacive limit to order–disorder. Strontium substitution can introduce additional anharmonicity to the on-site potential for Ti and thereby enhance the precursor effects [6]. However, the fact that pronounced order-parameter fluctuations in $(Ba_{0.8}Sr_{0.12})TiO_3$ are observed up to temperatures well below T_m' calls for an explanation different from that for $BaTiO_3$ where these fluctuations are not only weak but also restricted to temperatures above T_m' only.

It was pointed out in part I [8] that, because Sr has a smaller ionic radius than Ba has, Sr can take up off-centre positions similar to what is now well known for Li and Na ions in $KTaO_3$ [3, 4]. Such an off-centre Sr ion is a symmetry-breaking defect in the classification scheme of Halperin and Varma [20] since it lowers the symmetry locally. The off-centre occupancy of Sr ions will give rise to local dipoles which may in turn polarize their surroundings owing to the easy polarizability of the host ($BaTiO_3$) matrix above T_m'. We speculate that these clusters of polarized regions could be precursors to the cubic-to-tetragonal phase transition. The polarization clouds and associated effective dipole moment will increase in proportion to the softening of the host lattice on approaching T_m' from above. These are responsible for the intensity anomaly as well as the increasing electrorestrictive strain broadening. We feel that the increasing polarization clouds start to overlap at the temperature T_s at which the intensity anomaly disappears and probably all the Ti ions also become off-centre at the same temperature, i.e. T_s is the temperature at which the percolative-type transition occurs [21]. However, it remains unexplained why this percolative transition should occur at T_m' for $x = 0.08$ and at about 25 °C lower than T_m' for $x = 0.12$.

Minimization of the electrostatic energy associated with all Ti ions becoming off-centre requires [16] the formation of macroscopic structural domains below T_m' which limit the ferroelectric correlations to some macroscopic lengths. The random strains associated with the off-centre occupancy of Sr ions can, however, prevent perfect dipolar ordering within these structural domains owing to quadrupolar coupling and may lead to mesoscopic domains with a quadrupolar order parameter. In addition, the dipole–dipole interaction between randomly distributed Sr ions is expected to contribute a random component to the local fields. Such random fields may also lead to the formation of mesoscopic domains in accordance with the idea of Imry and Ma [12] within the larger structural domains. We feel that these mesoscopic domains are responsible for the observation of the low-frequency dielectric loss peaks in ϵ'' versus $\log f$ plots below T_m' discussed in parts I and II. Thus, although the $(Ba_{1-x}Sr_x)TiO_3$ samples for $x = 0.08$ and 0.12 are ferroelectric like macroscopically, the presence of mesoscopic domains and their relaxational freezing (as already discussed in parts I and II) suggest a similarity with an orientational glass state at a submicroscopic level. However, the frequency independences of T_m' and T_m'' as well as their equality for $x = 0.08$ and 0.12 is not consistent with a pure orientational glass state. As pointed out in parts I and II, for an orientational glass state, T_m'' should be significantly lower than T_m' and both should be frequency dependent, as is the case with compositions having $x > 0.12$. One is therefore led to conclude that, for strontium substitutions up to 12 at.%, the system has got mixed features corresponding to that of ferroelectric as well as the orientational glass state similar to what has been reported in $(K_{1-x}Li_x)TaO_3$ system also [4].

References

[1] Cox U J, Giband A and Cowley R A 1988 *Phys. Rev. Lett.* **61** 982
[2] Cox U J 1989 *J. Phys.: Condens. Matter* **1** 3565
[3] Höchli U T, Knorr K and Loidl A 1990 *Adv. Phys.* **39** 405
[4] Vugmeister B E and Glinchuk M D 1990 *Rev. Mod. Phys.* **62** 993
[5] Darlington C N W and Cernik R J 1991 *J. Phys.: Condens. Matter* **3** 4555
[6] Darlington C N W and Cernik R J 1992 *J. Phys.: Condens. Matter* **4** 4387
[7] Darlington C N W and Cernik R J 1993 *J. Phys.: Condens. Matter* **5** 5963
[8] Tiwari V S, Singh Neelam and Pandey D 1995 *J. Phys.: Condens. Matter* **7** 1441
[9] Stenger C G F and Burggraaf A J 1980 *J. Phys. Chem. Solids.* **41** 17
[10] Lifante G, Gonzalo J A and Windsch W W 1993 *Ferroelectrics* **146** 107

[11] Singh N and Pandey D 1996 *J. Phys.: Condens. Matter* **8** 4269
[12] Imry Y and Ma S K 1975 *Phys. Rev. Lett.* **35** 1399
[13] Waren B E 1969 *X-ray Diffraction* (New York: Addison-Wesley)
[14] Sawyer C B and Tower C H 1930 *Phys. Rev.* **35** 269
[15] Smolenskii G A 1970 *J. Phys. Soc. Japan (Suppl.)* **28** 26
[16] Pandey D 1995 *Diffusionless Phase Transitions in Oxides (Key Eng. Mater. 101–2)* ed C Boulesteix (Aedersmannsdorf: Trans Tech) p 177
[17] Bruce A D and Cowley R A 1981 *Structural Phase Transitions* (London: Taylor & Francis)
[18] Schmidt G 1990 *Phase Trans.* **20** 127
[19] Cross L E 1987 *Ferroelectrics* **76** 241
[20] Halperin B I and Varma C M 1976 *Phys. Rev.* B **14** 4030
[21] Rod S and Van der Klink J J 1994 *Phys. Rev.* B **49** 15 470